10-5-2016

Electrochemical Conversion of Biologically Produced Muconic Acid: Key Considerations for Scale-Up and Corresponding Technoeconomic Analysis

John E. Matthiesen
Iowa State University and Ames Laboratory

Miguel Suástegui
Iowa State University

Yutong Wu
Iowa State University

Mothi Viswanathan
Iowa State University, mothiv@iastate.edu

Yang Qu
Iowa State University, yqu1115@iastate.edu

See last page for additional authors

Electrochemical Conversion of Biologically Produced Muconic Acid: Key Considerations for Scale-Up and Corresponding Technoeconomic Analysis

Abstract

We present muconic acid, an unsaturated diacid that can be produced from cellulosic sugars and lignin monomers by fermentation, emerges as a promising intermediate for the sustainable manufacture of commodity polyamides and polyesters including Nylon-6,6 and polyethylene terephthalate (PET). Current conversion schemes consist in the biological production of cis,cis-muconic acid using metabolically engineered yeasts and bacteria, and the subsequent diversification to adipic acid, terephthalic acid, and their derivatives using chemical catalysts. In some instances, conventional precious metal catalysts can be advantageously replaced by base metal electrocatalysts. Here, we show the economic relevance of utilizing a hybrid biological–electrochemical conversion scheme to convert glucose to trans-3-hexenedioic acid (t3HDA), a monomer used for the synthesis of bioadvantaged Nylon-6,6. Potential roadblocks to biological and electrochemical integration in a single reactor, including electrocatalyst deactivation due to biogenic impurities and low faradaic efficiency inherent to side reactions in complex media, have been studied and addressed. In this study, t3HDA was produced with 94% yield and 100% faradaic efficiency. With consideration of the high t3HDA yield and faradaic efficiency, a technoeconomic analysis was developed on the basis of the current yield and titer achieved for muconic acid, the figures of merit defined for industrial electrochemical processes, and the separation of the desired product from the medium. On the basis of this analysis, t3HDA could be produced for approximately $2.00 kg –1. The low cost for t3HDA is a primary factor of the electrochemical route being able to cascade biological catalysis and electrocatalysis in one pot without separation of the muconic acid intermediate from the fermentation broth.

Keywords

3-Hexenedioic acid, Biorenewable chemicals, Cascade catalysis, Electrocatalysis, Electrochemical hydrogenation, Hydromuconic acid, Muconic acid, Nylon

Disciplines

Biochemical and Biomolecular Engineering | Bioresource and Agricultural Engineering | Organic Chemistry

Authors

John E. Matthiesen, Miguel Suástegui, Yutong Wu, Mothi Viswanathan, Yang Qu, Natalia Rodriguez-Quiroz, Adam Okerlund, George A. Kraus, D. Raj Raman, Zengyi Shao, and Jean-Philippe Tessonnier

Electrochemical Conversion of Biologically-Produced Muconic Acid: Key Considerations for Scale-up and Corresponding Technoeconomic Analysis

A paper published in ACS Sustainable Chemistry and Engineering

John E. Matthiesen,[1,2,3] Miguel Suástegui,[1,2] Yutong Wu,[1,2] Mothi Viswanathan,[2,4] Yang Qu,[2,5] Natalia Rodriguez-Quiroz,[1,2] Adam Okerlund,[2] George Kraus,[2,5] D. Raj Raman,[2,4] Zengyi Shao,[1,2] and Jean-Philippe Tessonnier[1,2,3,*]

[1]Department of Chemical and Biological Engineering, Iowa State University, 618 Bissell Road, Ames, Iowa 50011, United States

[2]NSF Engineering Research Center for Biorenewable Chemicals (CBiRC), 617 Bissell Road, Ames, Iowa 50011, United States

[3]US Department of Energy Ames Laboratory, 2408 Pammel Drive, Ames, Iowa 50011, United States

[4]Department of Agricultural and Biosystems Engineering, Iowa State University, 617 Bissell Road, Ames, Iowa 50011, United States

[5]Department of Chemistry, Iowa State University, 2438 Pammel Drive, Ames, Iowa 50011, United States

[*] Corresponding author

Abstract

Muconic acid, an unsaturated diacid that can be produced from cellulosic sugars and lignin monomers by fermentation, emerges as a promising intermediate for the sustainable manufacture of commodity polyamides and polyesters including Nylon-6,6 and polyethylene terephthalate (PET). Current conversion schemes consist in the biological production of *cis,cis*-muconic acid using metabolically engineered yeasts and bacteria, and the subsequent diversification to adipic acid, terephthalic acid, and their derivatives using chemical catalysts. In some instances, conventional precious metal catalysts can be advantageously replaced by base metal electrocatalysts. Here, we show the economic relevance of utilizing a hybrid biological–electrochemical conversion scheme to convert glucose to *trans*-3-hexenedioic

acid (*t*3HDA), a monomer used for the synthesis of bioadvantaged Nylon-6,6. Potential roadblocks to biological and electrochemical integration in a single reactor, including electrocatalyst deactivation due to biogenic impurities and low faradaic efficiency inherent to side reactions in complex media, have been studied and addressed. In this study, *t*3HDA was produced with 94% yield and 100% faradaic efficiency. With consideration of the high *t*3HDA yield and faradaic efficiency, a technoeconomic analysis was developed on the basis of the current yield and titer achieved for muconic acid, the figures of merit defined for industrial electrochemical processes, and the separation of the desired product from the medium. On the basis of this analysis, *t*3HDA could be produced for approximately $2.00 kg^{-1}. The low cost for *t*3HDA is a primary factor of the electrochemical route being able to cascade biological catalysis and electrocatalysis in one pot without separation of the muconic acid intermediate from the fermentation broth.

Introduction

Pyrolysis, fermentation, and chemical catalysis offer industrial routes to convert biomass to biobased chemicals. Advances in metabolic engineering have provided new microorganisms that are able to transform carbohydrates into diols (e.g., propanediol) and diacids (itaconic, succinic, fumaric, and malic acids) with high yields and titers.[1, 2] In parallel, new chemical catalysts have been developed to selectively convert glucose and lignin to platform chemicals through a broad range of liquid- and gas-phase reactions.[3, 4] Recently, hybrid conversion technologies have been developed to streamline chemical and biochemical transformations and/or enable more complex transformations.[5-9] Along these lines, cellulose was converted to ethanol and styrene through fast pyrolysis and subsequent fermentation of the levoglucosan intermediate.[9-11] Metabolically engineered yeast and bacteria also enabled

the production of triacetic acid lactone,[12, 13] which can be further converted to fuel additives, food flavoring agents, insecticides, and cosmetics using acidic and precious metal hydrogenation catalysts.[14] However, one major challenge of these hybrid technologies is the integration of two distinct process steps and the attendant complexity that integration entails. For example, phenolic byproducts produced during cellulose pyrolysis were shown to pose a strong inhibition to microbial growth.[9] In other instances, fermentation broths containing various biogenic impurities deactivated precious metal catalysts through reversible and/or irreversible poisoning.[7, 15, 16] Extensive separation and purification are therefore required to remove these compounds before downstream chemical conversion. [7, 15, 16] Streamlining the biological and chemical conversions in an integrated process currently remains a major challenge that will most likely require new catalysts and processes. One approach, which we have recently reported, entails the use of electrochemistry to mitigate the extensive separations that would be required for the conversion of biologically produced intermediates such as muconic acid (MA).[17, 18]

MA is a C_6 unsaturated dicarboxylic acid produced by the fermentation of cellulosic sugars and lignin-derived aromatics. In addition to recent efforts led by industry, in particular by Deinove[19] and Myriant,[20] several academic research groups have reported producing MA with high yields and titers using metabolically engineered bacteria: e.g., *Escherichia coli* reached 59.2 $g_{MA}\ L^{-1}$ at a 30% ($mol_{MA}/mol_{Glucose}$) yield,[21] and *Pseudomonas putida* achieved >15 $g_{MA}\ L^{-1}$ using the aromatic lignin monomer *p*-coumarate as a feedstock.[22] Recently, we have also demonstrated a 4-fold increase in MA titer using metabolically engineered *Saccharomyces cerevisiae* yeast, a model yeast that provides considerable advantages over its bacterial counterpart including resistance to bacteriophage contamination, impeller-induced

shear stress, and low pH.[17] These efforts have been motivated by MA's potential as a platform molecule to produce a vast array of renewable monomers of industrial importance, including adipic acid, terephthalic acid, caprolactone, 1,6-hexanediol, and 1,6-hexamethylenediamine.[18] Building blocks derived from MA are central to the manufacture of Nylon-6,6, polyethylene terephthalate (PET), and other polyesters, polyamides, and polyurethanes with an estimated global annual market greater than 22 billion U.S. dollars.[20, 23] In addition to its potential conversion to large-scale commodity chemicals, MA is also an intermediate to *trans*-3-hexenedioic acid (*t*3HDA), a promising monomer for the production of bioadvantaged nylons (Figure 1) and poly(ester)ethers: the additional double bond compared to adipic acid enables the subsequent functionalization of the polyamide, thus creating nylons with tailored properties.[17, 24, 25]

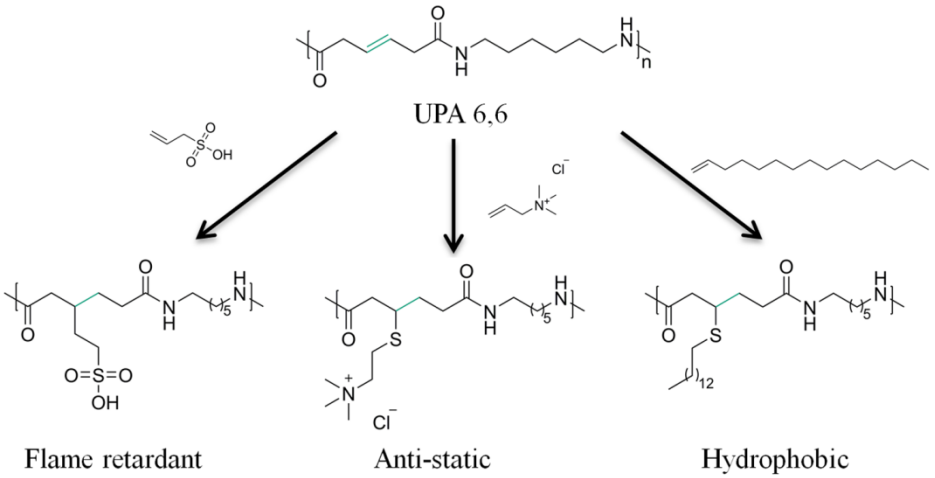

Figure 1. Potential commercial products derived from unsaturated polyamide 6,6 (UPA 6,6). The additional double bond (in green) in UPA 6,6 compared to Nylon 6,6 offers a site to incorporate new functional groups to synthesize advanced nylons with, for example, flame retardant, antistatic, and hydrophobic properties.

Currently, electrochemical hydrogenation (ECH) is the only means to produce *t*3HDA from MA with high selectivity and yields greater than 20%.[17, 18, 26, 27] As a result of the limited number of industrial electrochemical units in operation relative to conventional catalytic reactors, the development of a large-scale electrochemical process for the manufacture of biobased chemicals may be a deterrent to commercialization.[28, 29] Challenges associated with commercialization have been attributed to the lack of electrochemistry and electrochemical engineering education and the prohibitive cost for electrochemical synthesis.[29] However, this is not a fundamental obstruction for the commercialization of new electrochemical technologies. If the advantages of an electrochemical process outweigh its conventional counterpart, it becomes competitive. One example of industrial electroorganic synthesis currently in operation is the Monsanto process for the hydrodimerization of acrylonitrile to adiponitrile, a precursor to the diamine used in the synthesis of Nylon-6,6.[28] This approach produced nearly 400 000 metric tons of adiponitrile in 2014, or ∼30% of the adiponitrile market; the process appears competitive with the conventional route starting from butadiene.[30]

Here, we discuss the relevance of ECH for the downstream conversion of biologically produced intermediates. In an effort to scale-up the electrochemical synthesis of *t*3HDA and achieve economic viability, we detail nine important parameters outlined for organic electrosynthesis[28] and consider them in the context of the industrial production of *t*3HDA from MA. These include the following: the availability and cost of starting material, product yield, type and quantity of byproducts, separations, maximum cell current, energy consumption, the interference of the counter electrode, the chemical and electrochemical stability of the reactants and products, and the stability and availability of the cell

components.[28] Studying these parameters provides an outline for further scale-up as it will dictate the electrode potential, electrode material, electrolyte, temperature, pressure, and membrane or membraneless reactor design. We provide a technoeconomic analysis based on the results of the defined figures of merit, showing that the hydrogenation of MA to *t*3HDA is likely cost competitive with the production of adipic acid derived from petroleum.

Materials and Methods

Chemicals

Chemicals used in this study were purchased as follows: *cis,cis*-muconic acid (*cc*MA) (98%, Acros Organics); *trans,trans*-muconic acid (*tt*MA) (98%, Sigma-Aldrich); *trans*-3-hexenedioic acid (>98%, TCI); yeast nitrogen base without amino acids and ammonium sulfate, ammonium sulfate, adenine hemisulfate (Fisher Scientific); Synthetic Complete dropout lacking histidine, leucine, and uracil (MP Biomedicals). *cis*-3-Hexenedioic acid (*c*3HDA) was synthesized following previously reported methods[31] and used as a standard for quantification during electrochemical experiments (Figure S1). Specific details about *c*3HDA synthesis are found in the Supporting Information.

Electrochemical Conversion of MA Model Solutions

The electrochemical conversion of MA was characterized by cyclic voltammetry (CV) and bulk electrolysis by means of chronoamperometry (CA) and chronopotentiometry (CP). These investigations were conducted with a Bio-Logic VSP-300 potentiostat (Bio-Logic SAS, Claix, France) using a conventional three-electrode setup. Depending on experiments, either undivided or H-type glass cells were used as electrochemical reactors. For studies performed with model reaction media (e.g., MA in 0.1 M H_2SO_4 electrolyte), the

uncompensated solution resistance (R_u) measured by potentiostatic electrochemical impedance spectroscopy (PEIS) was compensated at 85% to obtain *iR* corrected potential on the working electrode. Compensation at 100% was not possible as it causes instability in potentiostat control.[32] Rotating disk electrode (RDE) experiments were performed using Pb embedded in Teflon and Pt working electrodes connected to a Pine modulated speed rotator set at 1600 rpm (Pine Research Instrumentation, Durham, NC). A platinum coil (Pine Research Instrumentation) and Ag/AgCl electrode (Bio-Logic) served, respectively, as the counter and reference electrodes. The solutions were purged with argon for 30 min before each measurement.

For bulk electrolysis, Pb (5N, ESPI metals), Fe, Ni, Sn, and Zn (The Science Company) electrode strips were used as working electrodes. Their corresponding surface areas are reported in Table S1. During the chronoamperometry experiments, samples of the reaction medium were taken at the specified reaction durations and analyzed using high pressure liquid chromatography (HPLC) and ^{1}H nuclear magnetic resonance (NMR).

Quantitative analysis was carried out by HPLC using a Waters Alliance system equipped with refractive index (RI) and photodiode array (PDA) detectors. Separation was achieved using a Bio-Rad Laboratories cation H^+ column kept at 30 °C. The collected samples (0.2 mL) were diluted 5 times with DI water prior to injection and analysis. Dilute sulfuric acid (5 mM) was used as the mobile phase at a flow rate of 0.3 mL min^{-1}. Reactants and products were quantified using the PDA detector set at a wavelength of 230 nm. Quantification of *cc*MA, *ct*MA, *tt*MA, *t*3HDA, *c*3HDA, and adipic acid was made possible through external calibration using solutions of well-known concentrations.

For ^{1}H NMR analysis, the samples were dried at room temperature, reconstituted in deuterium oxide, and analyzed with a Bruker 600 MHz NMR spectrometer (AVIII600).

Hybrid Microbial-Electrochemical Conversion

The strain *Saccharomyces cerevisiae* YSG50 (*MATa*; *ade2-1*; *ade3* Δ22; *ura3-1*; *his3-11,15*; *trp1-1*; *leu2-3,112*; *can1-100*) was engineered with the three-gene heterologous pathway to produce *cc*MA from 3-dehydroshikimic acid (DHS) and three genes ($aro4_{K229L}$, *TKL1*, and $aro1_{D1409A}$) to increase the accumulation of aromatic precursors from glucose. The genes were cloned into episomal vectors to enable the production of MA from glucose (Table S2). The strain YSG50-MA was cultured in Synthetic Complete dropout media lacking histidine, leucine, and uracil (SC-HLU, 0.5% ammonium sulfate, 0.16% yeast nitrogen base without ammonium sulfate and amino acids) in 2% glucose for seed growth and 4% glucose for the hybrid microbial–electrochemical conversion experiments. Two sequential overnight cultures were prepared before inoculation of the 50 mL undivided hybrid conversion reactor. A single colony was inoculated into 3 mL of SC-HLU medium, and after saturation, it was transferred into a 250 mL baffled flask containing 25 mL of the same selective medium. Both seed cultures were incubated in a shaker incubator at 250 rpm and 30 °C. Finally, the appropriate volume from the latter seed was transferred to the hybrid conversion reactor to initiate the fermentation with an optical density at a wavelength of 600 nm (OD) of 0.2. The reactor was then placed in a water bath at 30 °C on top of a stirring plate to maintain aeration at 250 rpm. After 72–74 h fermentation, the electrodes were immersed in the broth, and a −1.5 V potential was applied to the working electrode to convert biologically produced *cc*MA to *t*3HDA. Samples (1 mL) were collected at 24, 48, 72, 72.5, 73, 73.5, 74, and 96 h and analyzed by ^{1}H NMR with a dimethyl sulfoxide standard.

Cell Viability Assays

To assess the effect of metal leaching, cultures were grown in a 96-well plate in growth medium containing 2.5 vol/vol % of an aqueous metal concentrate. These solutions were prepared for each metal by placing the corresponding electrode in aqueous acetic acid at pH 3 (mimicking fermentation conditions) at the open circuit voltage for 5 min, followed by evaporation and reconstitution in water. The OD of the cultures was monitored using a Synergy 2 Multi-Mode plate reader (Winooski, VT); the exponential phase curves were used to calculate the specific growth rates.

To assess the effect of the applied potential during hybrid conversion, 1 mL samples were taken before and after the electrochemical process. The samples were diluted in sterile water to a cell OD of 10^{-4} and plated on the selective media. The plates were incubated for 2 days at 30 °C, and the colonies were manually counted.

Separations

Following electrochemical processing, *t*3HDA was separated from the spent fermentation broth using carbon filtration and crystallization modified from a method we reported previously.[17] In short, the pH of the cell-free broth was first brought from 3 to 8.5 with 10 M NH_4OH to increase the solubility of HDA. The basic solution was then concentrated by vacuum evaporation and filtered over a 15 mm deep Norit CN1 activated carbon bed (preconditioned with 10 mM NH_4OH) to remove soluble impurities including color bodies, cell lysis products, proteins, and amino acids. The obtained filtrate was brought to pH 1.5 using 18.4 M sulfuric acid and crystallized at 4 °C overnight. *t*3HDA crystals were recovered by vacuum filtration with a Whatman 50 filter, washed with 4 °C 10 mM sulfuric acid, and placed in a desiccator to dryness. The purity of the recovered *t*3HDA was

calculated on the basis of its ^{1}H NMR spectrum. Trace elements in the sample were quantified by inductively coupled plasma optical emission spectroscopy (ICP-OES) using a Perkin-Elmer Optima 8000 instrument.

Technoeconomic Analysis

A technoeconomic analysis (TEA) was developed on the basis of estimated yields at each process stage (fermentation, electrochemical conversion, and separations), literature values, and personal communications with electrochemical companies. While multiple design parameters are defined, the process development is still in the early stages. As opposed to SuperPro Designer (Intelligen, Inc., Scotch Plains, NJ), an early stage TEA (ESTEA) was chosen to estimate the cost of producing chemicals from sugar.[33, 34] ESTEA is a Microsoft Excel-based technoeconomic model for economic analysis at the early stages of process development when many parametric values are only known at a relatively low degree of certainty. For example, SuperPro Designer requires approximately eight inputs per unit operation, some of which are often not known and require estimation during early stage analysis. In contrast, the ESTEA model only requires three, typically known, parameters.[34] To compensate for the simplified, lumped-parameter approach of ESTEA, we use a Lang Factor that translates the capital cost for a specified unit operation into a total capital cost for that function. We selected a Lang Factor of 5, per Dysert.[35] The prior version of ESTEA had not included the ability to cost-estimate electrocatalysis. Therefore, in this model, we added in the capability to estimate costs for electrocatalysis based on a personal quote for the purchase of a two-electrode undivided reactor with a Pb cathode and a platinized TiO_2 anode.[29, 36] Additional details can be found in the Supporting Information. To provide economic context, we searched online vendors for the prices of *t*3HDA and closely related

compounds. We were unable to find large-scale pricing on *t*3HDA besides Sigma ($14.10 g^{-1}). While the values pricing the bulk production of *t*3DHA are unknown, adipic acid, a closely related compound with current market values in the range $1.60–1.70 kg^{-1},[26, 37] was used as a reference point.

Results and Discussion

Integration of Microbial and Electrochemical Conversions

Biocatalysis represents an attractive approach for producing complex platform chemicals that can be subsequently upgraded and diversified using chemical catalysts. Combining fermentation and conventional heterogeneous catalysts generates, however, new challenges that need to be addressed before scale-up and commercialization of these hybrid processes.[7, 15] In particular, fermentation media are complex mixtures containing a wide range of nutrients, including salts, vitamins, amino acids, and trace elements, required for microbial growth and the production of the target chemical. During fermentation, various biogenic impurities are also produced because of microbial activity and cell lysis. Many of these nitrogen- and sulfur-containing proteins, amino acids, and metabolites are problematic for conversion processes as they poison precious metal catalysts (Pd, Pt, Rh, Ru) through reversible and irreversible binding. These undesired effects are observed at low concentration. For example, Ru/C used to hydrogenate biologically produced lactic acid to propylene glycol was irreversibly poisoned by cysteine and methionine, two common amino acids, at levels of 100–150 ppm.[38] Therefore, extensive separation and purification of the platform intermediate is usually required before further upgrading, which significantly

increases the cost of the target chemical. Indeed, complex separations can contribute up to 60% of the overall cost for sugar-derived fermentations.[39]

We have recently demonstrated that electrocatalysis provides unique opportunities to streamline microbial fermentation and downstream catalytic upgrading.[17] Common electrocatalysts include late and post-transition metals that are significantly less susceptible to deactivation than conventional transition metal catalysts.[18] As a result, it was possible to electrochemically hydrogenate MA directly in the fermentation broth, in the presence of all biogenic impurities. The studied sequential process, which involved MA production from glucose using an engineered strain of *S. cerevisiae* with the highest titer in yeast (559.5 mg L^{-1}) followed by ECH of the acidified broth (pH 2.0), resulted in 98% selectivity to *t*3HDA at 96% MA conversion.[17] The ECH step was repeated 5 times without any noticeable alteration of the catalytic activity. In addition, it is worth noting that the electrochemical step was performed under ambient conditions and that hydrogen was produced *in situ* directly from the broth.

To identify other potential catalysts able to convert MA directly in the fermentation medium, decrease space-time, and reduce the number of processing steps during the conversion of glucose to *t*3HDA, cascade catalysis was attempted in the present study. Cascade catalysis entails combining various chemical conversion steps in one pot without the isolation of the intermediates.[8] Five metals were selected on the basis of their relevance in industrial electrochemical processes.[28] For these studies, batch fermentation using the engineered strain *S. cerevisiae* YSG50-MA proceeded for a total reaction time of 96 h. The relatively low pH of the broth triggered the spontaneous transformation of biologically produced *cis,cis*-muconic acid (*cc*MA) to its corresponding *cis,trans* isomer (*ct*MA), in good

agreement with previous observations.[18, 23, 40] The reference, working, and counter electrodes were immersed in the broth after 72 h of fermentation, and a potential of −1.5 V versus Ag/AgCl was applied to the working electrode for 2 h to electrochemically hydrogenate *ct*MA to *t*3HDA. As shown in Figure 2, *ct*MA derived from the fermentation broth was converted to *t*3HDA on Fe, Sn, Pb, and Zn working electrodes.

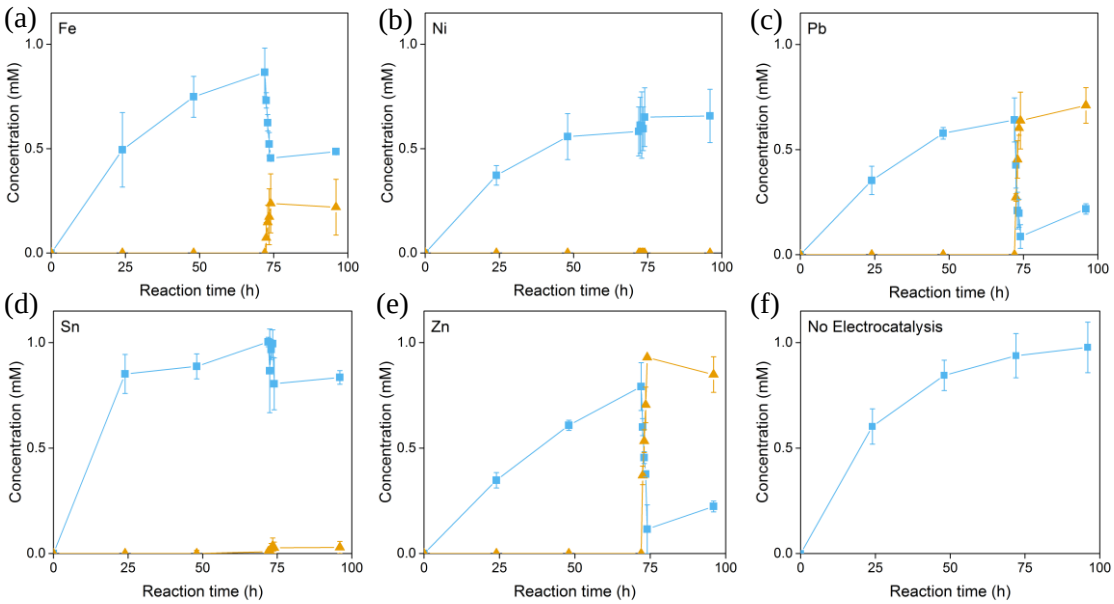

Figure 2. Concentrations of *ct*MA (■) and *t*3HDA (▲) during the simultaneous fermentation and ECH using (a) Fe, (b) Ni, (c) Pd, (d) Sn, (c) Zn electrodes, and (f) in the absence of an electrocatalyst. The displayed results correspond to averaged duplicates. The error bars reveal variations in *ct*MA titer due to changes in stirring rate with reactor location on the multiple positions stirring hot plate. Fermentation proceeded for 96 h and the electrochemical hydrogenation took place between 72 and 74 h.

Ni displayed no conversion likely due to the strong adsorption of biogenic impurities containing nitrogen and sulfur.[38, 41] Similarly, Sn and Fe displayed minimal conversion due to the competitive hydrogen evolution reaction (HER) and poisoning from biogenic impurities in the solution. The platinum counter electrode, although a precious metal, did not show any sign of poisoning under these reaction conditions. Interestingly, besides *ct*MA and *t*3HDA

observed by ^{1}H NMR under these conditions, no significant change occurred to the other species present in the fermentation broth (Figure 3). After 2 h of electrochemical conversion, *ct*MA continued to increase, suggesting the applied potential under these specific conditions did not significantly impact cell viability.

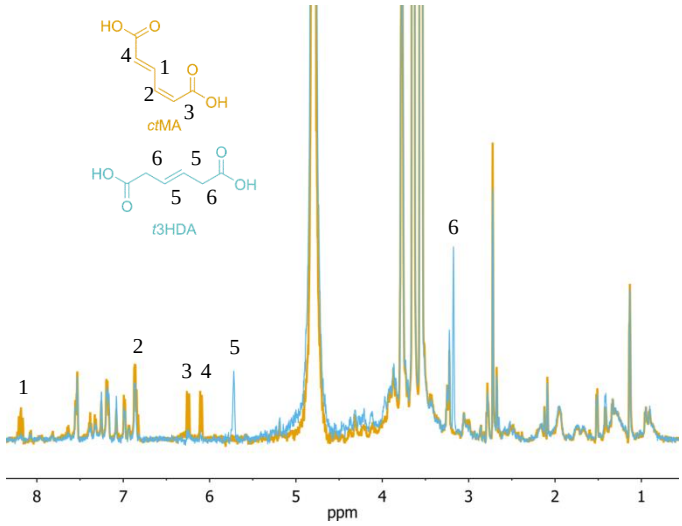

Figure 3. ^{1}H NMR (600 MHz, D_2O) spectra of the fermentation broth samples collected before (orange) and after (blue) the electrochemical hydrogenation. During the 2 h reaction, the signals for *t*3HDA increase while *ct*MA decreases as a result of its hydrogenation. The extraneous signals do not change.

For the determination of the influence of applied potential on the engineered microbe, yeast cells were sampled before and after the electrochemical conversion, cultured on Petri dishes, and counted. This study did not reveal any correlation between the metal used and the change in viable cell count (Figure 4a). It appears that the cell count was not influenced by the charge (electric current) transferred through the solution during ECH either (Figure 4a). However, additional optical density (OD) measurements suggested that cell growth was discouraged due to metal ions leaching into the solution before a cathodic potential was applied. The Pourbaix diagrams of the various metals tested in this work confirmed that that

the corresponding dicationic metal ions are the thermodynamically favored species under open circuit voltage.[42] In the absence of an applied cathodic potential, the studied metals underwent a redox reaction with protons in solution (corrosion), and M^{2+} ions were leached from the working electrode into the broth. Leaching can be minimized by applying the desired potential within seconds after the working electrode is immersed in the solution. Therefore, leaching would most likely not affect the long-term stability of the reactor.

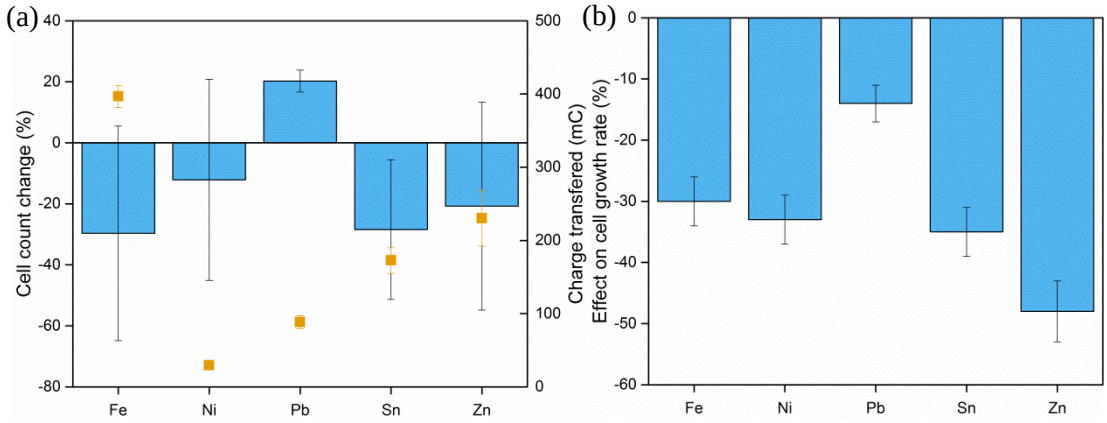

Figure 4. Effect of ECH on cell count (a). Significant changes were not observed for the studied metals (bars) and charges transferred during the 2 h reaction (scatter). Metal ions leached in the absence of an applied cathodic potential did impact the specific cell growth rate (b).

The effect of metal ions on cell growth was further investigated using model solutions. Specifically, the metal electrodes were placed in a solution at pH 3, similar to the acidity of the studied broth, and the corresponding corrosion reaction was allowed to proceed for 5 min. The obtained solutions were evaporated, reconstituted in water, and used to spike the yeast growth media with metal ions. OD measurements revealed that the specific cell growth rate decreased in all cases when 5 µL of the metal ion solution was added to 200 µL of growth medium (Figure 4b). Lead showed the least detrimental effect with a reduction of only ~15% of specific growth rate relative to the control experiment. In contrast, zinc caused

the most significant drop in specific growth rate with a 45% reduction. Additional experiments to accurately determine the metal corrosion rates in fermentation broths and the levels at which the metal ions become toxic to the yeast cells were not performed as these studies would clearly be beyond the scope of the present work. Yet, our results suggest lead is the most promising metal for integration of the microbial and electrochemical conversions in a single reactor and ECH can be performed in a cascade fashion without separation of the *ct*MA intermediate.

Electrochemical Studies and Considerations for Scale-Up

In addition to investigating the compatibility of the microbial and electrochemical conversions as a prerequirement for future integration in a simultaneous cascade process, it is also important to gain further insights into the electrochemical reaction to optimize it. Experiments performed on model solutions provide an understanding of how reaction rates, selectivities, and faradaic efficiencies are impacted by the applied potential and electrochemical reactor design (e.g., cell geometry). This part of the work is critical for the subsequent technoeconomic analysis and for the determination if ECH is technically feasible and economically viable at an industrial scale.

Cyclic voltammetry was performed to determine the onset potential for *ct*MA hydrogenation and gain insights into competing reactions. Similar to previous studies, Pb was chosen as the catalyst because of its large hydrogen overpotential and ability to convert *ct*MA directly in the fermentation medium with minimal cell death. As shown in Figure 5a, Pb is able to convert *ct*MA at a cathodic potential of −0.6 V versus Ag/AgCl, about 0.3 V above the cathodic potential required for proton reduction on Pb. Increasing the concentration of the reactant only yielded higher current (Figure 5a). Additional measurements performed with

aqueous solutions of *t*3HDA demonstrated that the *ct*MA hydrogenation product is stable and does not adsorb onto the catalyst surface; the polarization curves for the blank electrolyte and product were found to be similar even at a high *t*3HDA concentration (Figure 5b). Protons in the solution are the only other electroactive species within the potential window.

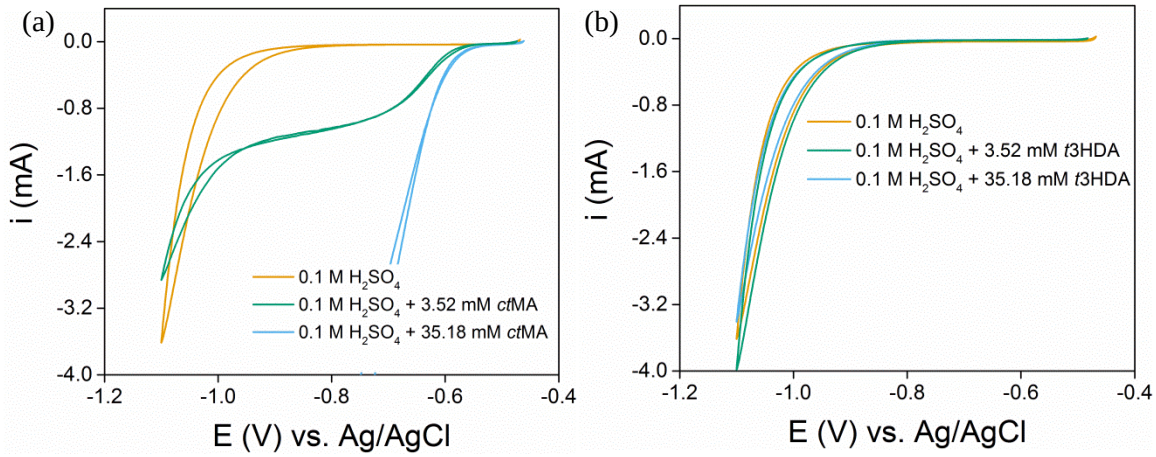

Figure 5. Cyclic voltammograms for the 0.1 M H_2SO_4 with and without *ct*MA using a Pb RDE at 50 mV s^{-1} (a) and 0.1 M H_2SO_4 with and without *t*3HDA (b). *ct*MA displays a reduction peak at -0.6 V while *t*3HDA does not display any electron transfer.

Bulk electrolysis offered further useful information for electrochemical cell design. While the ECH has been studied so far at low *ct*MA concentration (<1 g L^{-1}), it is important for future process scale-up to also examine the reaction using concentrated feed stream in multiple cell configurations. An undivided cell and H-cell delineated the differences between cell configurations and the corresponding influence on selectivity and faradaic efficiency. With application of a potential of −0.8 V to a 5 g L^{-1} solution of *ct*MA in 0.1 M H_2SO_4 electrolyte using a 5 cm^2 Pb electrode strip, 92% MA conversion and 90% selectivity to *t*3HDA were achieved in an unpurged and undivided cell (Figure 6a). Interestingly, *t*3HDA was consumed to a minor extent over the course of the reaction. Product degradation in the

undivided cell likely occurred on the counter electrode or in the solution as the cathodic polarization curves recorded for *t*3HDA solutions suggest no additional electron transfer (Figure 5b); i.e., *t*3HDA does not further react at the cathode. The loss in *t*3HDA selectivity was further investigated by cyclic voltammetry using a Pt rotating disk electrode (RDE) to represent the counter electrode during the reaction. As shown in the corresponding polarization curves, an oxidation peak is observed at 0.7 V versus Ag/AgCl (Figure 7a). In addition, bulk electrolysis using the Pt coil working electrode using 5 g L^{-1} *t*3HDA at the highest required current demand during the electrochemical conversion in Figure 6a (70 mA) did not show any significant differences in the ^{1}H NMR spectra before and after the chronopotentiometric experiment of *t*3HDA (Figure 7b). This suggests that *ct*MA or intermediates during the conversion to *t*3HDA react with other compounds to cause the decrease in selectivity observed in Figure 6a. However, further study of potential *t*3HDA oxidation will require additional bulk electrolysis experiments, which will determine if a membrane or separator needs to be added to the electrochemical cell.

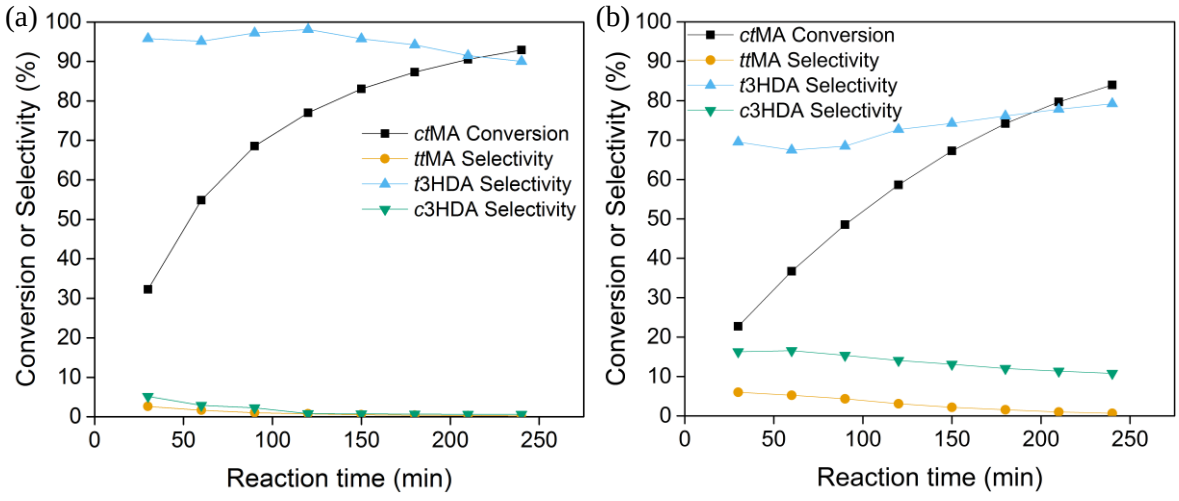

Figure 6. Electrochemical hydrogenation of 5 g L^{-1} *ct*MA in 0.1 M H_2SO_4 in an (a) undivided cell and (b) H-cell. Significant differences in product selectivities are observed depending on cell configurations.

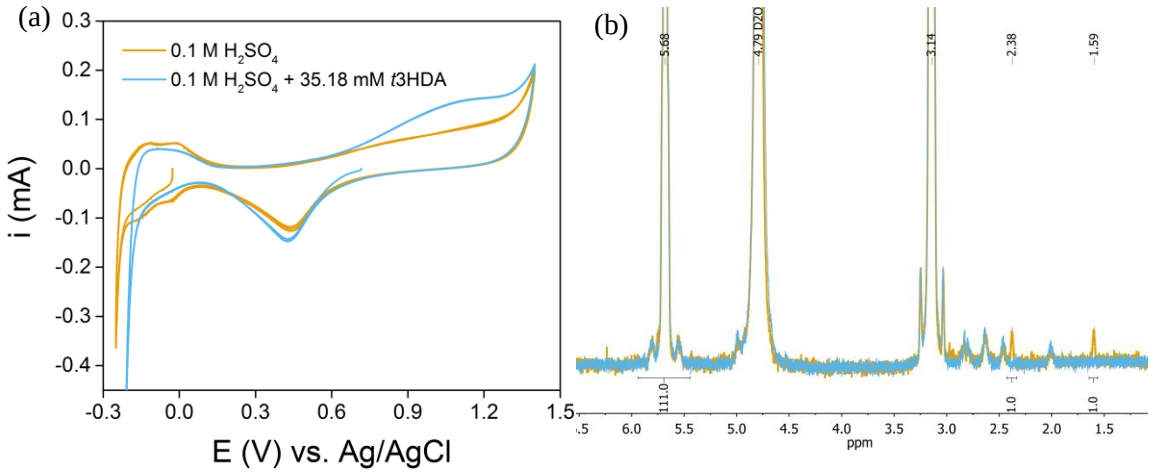

Figure 7. Cyclic voltammograms using a Pt RDE at 50 mV s^{-1} of an electrolyte containing 0.1 M H_2SO_4 and a solution containing 35.18 mM *t*3HDA in 0.1 M H_2SO_4. A new oxidation peak is observed at 0.7 V in the presence of *t*3HDA (a). ^{1}H NMR (600 MHz, D_2O) spectra collected before and after a 4 h chronopotentiometric experiment of 35.18 mM solution of *t*3HDA in a 0.1 M H_2SO_4 solution using a Pt coil working electrode at 70 mA (b). 70 mA corresponds to the largest demand the counter electrode is required to provide. Before reaction: blue; after 4 h reaction: orange. Minor traces of adipic acid (4H 2.38ppm, 4H 1.59ppm) and extraneous compounds are observed after 4 h, however, these are likely too small to be representative of the degradation observed in Figure 6 as proton integration correspond to a 111:1 difference in concentration between *t*3HDA and adipic acid.

The effect of cell configuration on conversion, selectivity, and faradaic efficiency was further studied by performing the electrochemical reaction in an H-cell. With this shift, more capital is required to set up and maintain the membrane or fine frit used to separate the two cell compartments.[28] After a 4 h electrochemical conversion with Pb using an H-cell, a significant quantity of *cis*-3-hexenedioic acid (*c*3HDA) was produced compared to *t*3HDA while product degradation was kept to a minimum (Figure 6b). *c*3HDA was likely formed as a result of the changes in pH in each cell. Considering that the pH would be higher in the cathode compartment of the H-cell, we could favor the kinetic product over the thermodynamic product.[18] Although the tunable reaction conditions are interesting, polymer

synthesis typically requires pure isomers and not a mixture of *cis* and *trans* molecules for synthesis. For this reason, we decided to continue utilizing the undivided cell to interrogate the industrial feasibility of the ECH reaction.

In addition to high product yields, it is important to consider the energy consumption of the process. For the conversion of 1 mol *ct*MA (142 g mol^{-1}) at 100% faradaic efficiency, 192 970 C are required. Currently, the relatively low *ct*MA concentration, although being representative for direct conversion of MA in the yeast fermentation broth (559 mg L^{-1}), limits the faradaic efficiency of the electrochemical hydrogenation due to the large concentration difference between protons and the organic reactant.[18, 43] Hence, hydrogen recombination to form H_2 gas through the hydrogen evolution reaction (HER) is difficult to prevent. Increasing the concentration of *ct*MA to a level close to its solubility limit (5 g L^{-1} under acidic conditions) allowed the hydrogenation in 0.1 M H_2SO_4 to achieve a 90% faradaic efficiency below 10% conversion utilizing both an undivided cell and H-cell (Figure 8a). Although not common for industrial electrocatalytic processes, the electrolyte was also purged with Ar for 30 min before and during the reaction duration to examine the effects of dissolved gases in the reaction medium, particularly oxygen.[28] By purging the cell with Ar before and during the reaction, a faradaic efficiency of ~100% was achieved showing that dissolved gases in model solution were the only other electroactive species (Figure 8a). Although this did not prevent product degradation completely, the lower amount of current the counter electrode is required to provide decreased the amount of *t*3HDA consumed (Figure 8b).

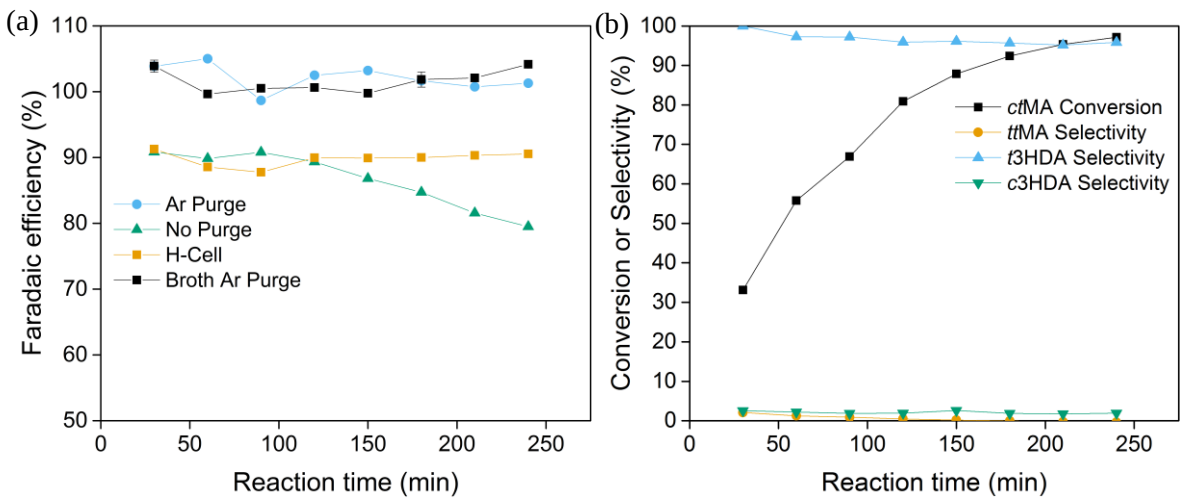

Figure 8. Faradaic efficiencies achieved using an undivided cell (with and without Ar purge), H-cell (without Ar purge), and undivided cell with spent fermentation broth (a); electrochemical conversion of *ct*MA in an undivided cell purged with Ar before and during the reaction (b).

With an increase in the complexity from the studies with the model solutions, 5 g L^{-1} of *ct*MA was hydrogenated directly in a spent fermentation broth with an added 0.1 M H_2SO_4 electrolyte purged with Ar for 30 min before and during the reaction. As shown in Figure 9, *ct*MA was hydrogenated at a similar rate to that for the model solutions. In addition, the increase in *t*3HDA selectivity over the course for the reaction suggests that the impurities present in the fermentation broth actually prevent the degradation of the product *t*3HDA, in good agreement with previous observations.[17] Interestingly, the faradaic efficiency for the electrochemical conversion directly in the spent media was still ~100%. This, again, suggests that the only substantial electroactive species in the spent media under the applied potentials at the working electrode is *ct*MA and not any other extraneous compound present in the spent fermentation broth. It should also be noted that *t*3HDA's solubility limit under acidic conditions (~11 g L^{-1}) prevents its precipitation over the course of the reaction.

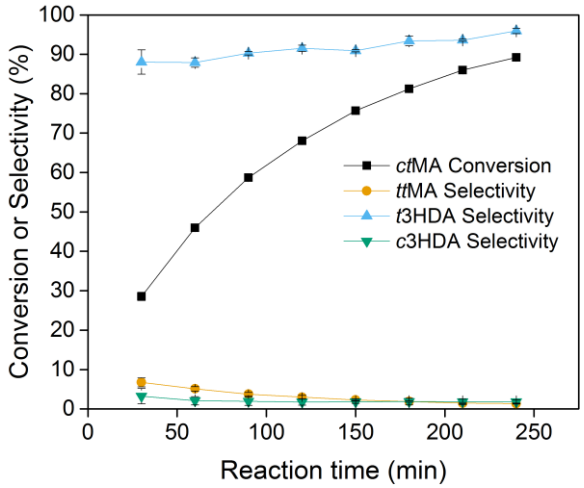

Figure 9. Bulk electrolysis of 5 g L^{-1} solution of *ct*MA in 0.1 M H_2SO_4 electrolyte purged with Ar using a Pb working electrode. No loss in selectivity of *t*3HDA was observed during the reaction.

In addition to the faradaic efficiency, product and reactant stabilities, and the cost/availability of feedstocks, the cell current density is another important factor to be considered for scale-up. For example, the current density of the Monsanto process has been reported to be 0.2 A cm^{-2}, limiting the rate of adiponitrile production to 0.01 mol m^{-2} s^{-1} at a 100% faradaic efficiency. With consideration of the capital costs for an electrochemical flow cell being around 10 000 to 20 000 USD per m^2,[36] the production rate could be limited by the ability to purchase enough surface area for the reaction to take place on. The average current density for the conversion of *ct*MA on the previous experiments was only 0.004 mA cm^{-2}, which is primarily due to the relatively low solubility of *ct*MA at room temperature in acidic media. To increase the current density while maintaining the ability to perform cascade catalysis, more reactant could be solubilized using a cosolvent such as ethanol, the reaction mixture could be heated, or the applied cathodic voltage would need to increase. However, each of these methods have trade-offs due to cosolvent costs, the need for process heat, and an increase in voltages that reduce the faradaic efficiency. To simplify the technoeconomic

analysis and stay within the limits of our potentiostat, the use of cosolvent, process heat, and higher applied cathodic voltages were not considered. Additionally, the technoeconomic analysis (*vide infra*) showed that major improvements in the electrochemical process would not significantly influence the overall cost of *t*3HDA relative to the upstream expenditures.

Separations

Separation of *t*3HDA from the spent fermentation broth was achieved utilizing carbon filtration and crystallization at low pH.[17] In this work, ammonium hydroxide was used to solubilize *t*3HDA after the electrochemical conversion rather than sodium hydroxide due to the higher solubility limit of the sulfate salt (42.9 mass% vs 16.13 mass% at 20 °C).[44] The higher solubility of ammonium sulfate allows for the additional evaporation of solvent from the post carbon filtration solution prior to lowering the pH with sulfuric acid. The smaller volume during batch crystallization lessens the loss of *t*3HDA to the mother liquor which in turn increases the yield of *t*3HDA in crystalline form. ^{1}H NMR analysis showed that the collected *t*3HDA was pure at 98%. Further elemental analysis by ICP-OES revealed that trace elements derived from the fermentation broth Ca and Mg represent less than 0.4 wt % of the purified *t*3HDA sample, while K and Na accounted for only 0.03 wt % (Table S3). Other metals potentially derived from the ECH or fermentation media (Cu, Fe, Pb, Pt, and Zn) were below detection limits. Although inorganic impurities were present in the sample, they did not inhibit the polymerization process, as demonstrated previously.[17]

Technoeconomic Analysis

For development of the early stage TEA, a process flow diagram was developed (Figure 10). In this process, feedstock is fermented to produce MA, which is then subjected

to an electrochemical conversion to produce *t*3HDA after the removal of cell mass. The location of the centrifugation step to remove cell mass could occur before or after the electrochemical conversion. No additional separations of other biogenic impurities are required as the Pb electrode is stable in the presence of all impurities present in the spent fermentation media, including cells and cell lysis products. After the electrochemical conversion, *t*3HDA is separated from the spent fermentation broth though adsorption and crystallization processes.

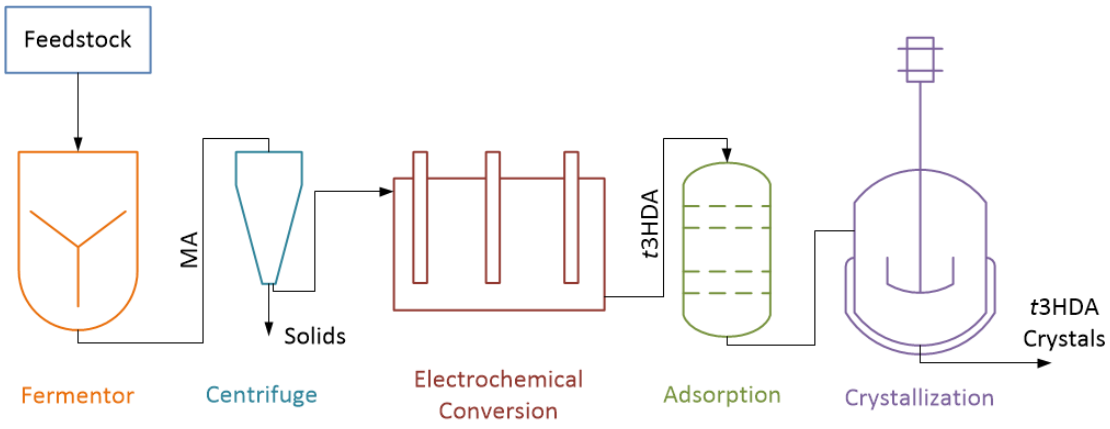

Figure 10. Anticipated overall process flow diagram to produce *t*3HDA from sugar, based upon lab-scale efforts. Propagation tanks, wastewater treatment, and other ancillary functions are not shown but are accounted for in the TEA.

To scale the process to its industrial size, key economic and sizing parameters based on other commercialized biobased processes as shown in Table 1 were selected. The process input parameters, classified through unit operations, are provided in Table 2. The plant size was chosen as 3% of the approximate annual adipic acid market size, or 83 kTons year^{-1}, and reflects other biobased fermentation processes that are coming online.[30, 45, 46] Feedstock was assumed from USDA's historical raw sugar pricing data at \$0.30 kg^{-1}. Productivity, titer, and yield for the fermentation correspond to the values obtained for metabolically engineered *E.*

coli, a microbe that received significantly more attention than *S. cerevisiae*.[21] Preliminary experiments indicated that both biocatalysts are equally compatible with the subsequent electrochemical hydrogenation. The total installation costs for all the equipment were calculated using a Lang factor of 5. This total capital charge was then amortized at 10% for 10 years. Taxes, depreciation, and salvage values were ignored in this analysis. The plant was assumed to operate for 330 days annually.

Table 1. ESTEA: Economic and plant sizing parameters for conducting TEA

Parameter	**Value**	**Reference**
Plant size (kT $year^{-1}$)	83	[47]
Feedstock (\$ kg^{-1})	\$0.30	[48]
Operating days (days $year^{-1}$)	330	[49]
Internal Rate of Return (IRR) ($year^{-1}$)	10%	[50]
Lang Factor	5	[35]

Table 2. ESTEA input process parameters for conducting TEA

Parameter	**Value**	**Reference**
Fermentation		
Productivity (g L^{-1} h^{-1})	1.1	[21]
Titer (g L^{-1})	59	[21]
Yield (g g^{-1})	23%	[21]
Electrochemical Conversion		
Solubility	5 g L^{-1}	
Selectivity	96%	
Conversion	98%	
Separations-Adsorption		
Freundlich Coefficient	10	
Freundlich Exponent	0.80	
Yield	98%	
Purification-Crystallization		
Purity	98%	
Yield	98%	
Separating Agent	H_2SO_4	

The results of TEA are shown in Figure 11. ESTEA estimated the cost of producing *t*3HDA at \$2.13 kg^{-1}. As shown in Figure 11a, the distribution of costs is typical of large, mature bioprocesses, with feedstock comprising more than half of the total production cost. Fermentation is the dominant unit operation cost, followed by purification (adsorption and crystallization) (Figure 11b). The estimated electricity costs, based on experimental data, are \$1.26 M annually, a large number until it is contextualized on a unit product mass basis, yielding under \$0.02/kg. The total costs associated with the electrochemical conversion operation including capital, labor, and operations (electricity, electrodes) are low, a mere 5% of nonfeedstock costs, and less than 4% of the total overall cost, due to the relatively inexpensive electrodes and high yields associated with the particular electrochemical conversion. While the electrochemical conversion process accounted for a minimal amount of the entire process, the ability to cascade reaction steps caused an approximately 8% decrease in the estimated cost of separations prior to the electrochemical conversion.[51]

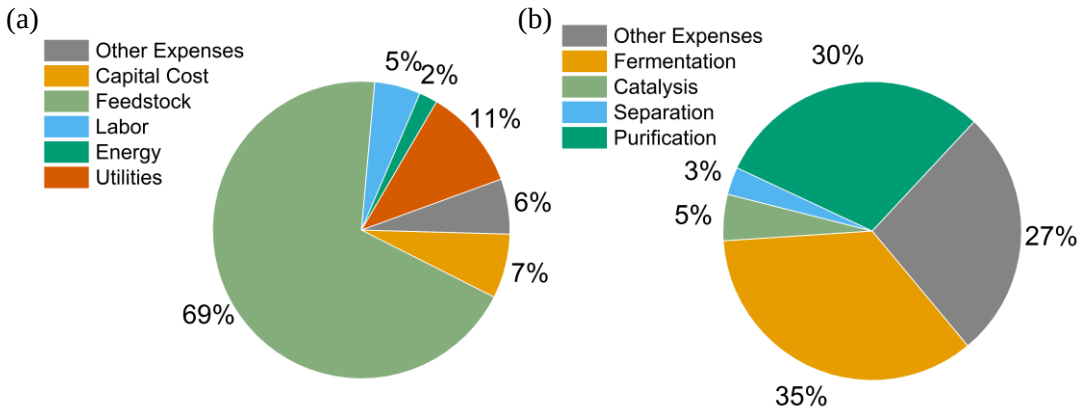

Figure 11. Distribution of the \$2.13 kg^{-1} MSP between the major cost categories of feedstock, capital, labor, energy, utilities, and other expenses; feedstock is dominant (a). Distribution of the nonfeedstock cost components (capital, labor, energy, and utilities) between the unit operations for the process (b).

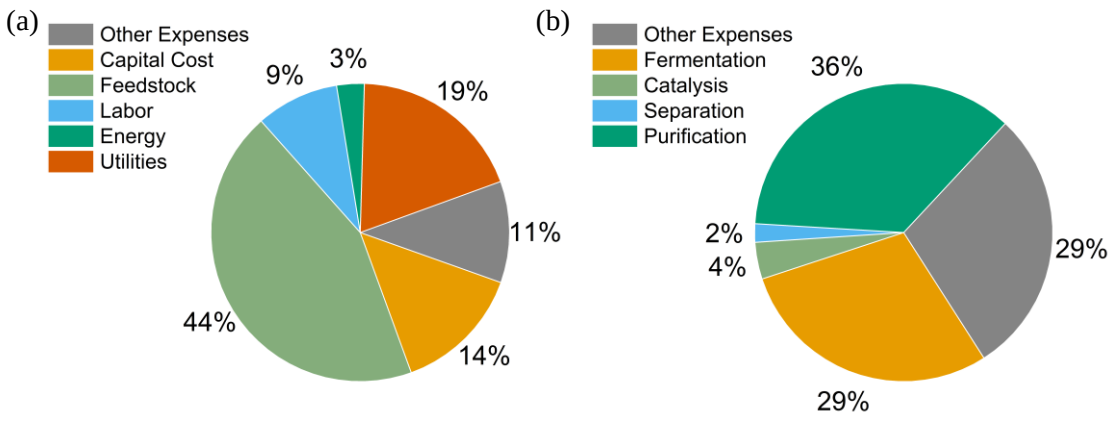

Figure 12. Distribution of the \$0.98 kg^{-1} MSP, an optimistic scenario, between the major cost categories of feedstock, capital, labor, energy, utilities, and other expenses; feedstock is dominant (a). Distribution of the nonfeedstock cost components (capital, labor, energy, and utilities) between the unit operations for the process (b).

The relatively high feedstock cost makes stage yields critical. For example, the sensitivity coefficient of MSP to fermentation yield is 1.0, that is, a 1% change in fermentation yield ($g_{MA}/g_{glucose}$) causes a 1% change in MSP. If the fermentation yield is raised to the theoretical limit of 79% $g_{MA}/g_{glucose}$ (which assumes glucose is stoichiometrically converted to MA), the estimated MSP decreases to \$0.98 kg^{-1} (Figure 12), which is competitive with the market price for benzene-derived adipic acid. Additionally, if the feedstock is changed to a lower value chemical, such as lignin,[22] the process economics will improve considerably. Considering recent advances in developing metabolic routes to MA with increased titers and yields and using other feedstocks, the large portions of the processing costs will greatly decrease. As a result, future prospects for MA use are promising.[23, 52, 53]

Considerations for *t*3HDA Adoption

The adoption of a new molecule by the chemical industry is primarily driven by end user demand, market size, and production costs. However, in the case of direct replacement

chemicals, their implementation can be significantly hampered due to risks associated with the volatility in oil prices, changes in existing processes to accommodate the new compound, and the absence of information on the toxicity of the new chemical. As a result, time scales on the order of 5–10 years are common for the introduction of a new chemical to the marketplace. *t*3HDA presents here several advantages over other biobased products that are detailed below.

Cost

Our technoeconomic analysis indicates that *t*3HDA can be produced at a reasonable cost of approximately \$2.00 kg^{-1} as a result of the streamlined process combining fermentation and electrochemical hydrogenation. As already discussed in the previous section, this MSP is comparable to adipic acid.

Market

When blended with adipic acid, *t*3HDA enables the synthesis of bioadvantaged nylons, i.e., polyamides in which new functionalities are introduced by cross-linking or functionalization of *t*3HDA's carbon–carbon double bond. Therefore, *t*3HDA does not replace but instead complements adipic acid for nylon production. We have also shown that *t*3HDA can be blended with adipic acid in any ratio ranging from 1% to 99%, thus allowing an accurate control of the degree of unsaturation in the obtained polyamide.

Implementation

The same procedure was used to synthesize Nylon-6,6 (with 100% adipic acid) and unsaturated polyamide 6,6 (with 100% *t*3HDA), thus demonstrating that *t*3HDA can be implemented in existing processes for Nylon-6,6 production.

Toxicity

The toxicity of *t*3HDA has already been evaluated. The U.S. Environmental Protection Agency has approved its utilization (*t*3HDA is listed in the Toxic Substances Control Act, TSCA, Chemical Substance Inventory), and regulatory information is available.

Chemistry

Unsaturated diacids, in particular, maleic and fumaric acids, are used in industry for the production of unsaturated polyester resins.[54] Techniques for cross-linking and derivatization of these polymers using the unsaturation have been developed and can be extended to *t*3HDA.

Conclusions

Although a combination of biological and chemical conversions expands the range of biobased chemicals accessible from glucose, the integration of fermentation and heterogeneous catalysis in a single hybrid process generates significant challenges due to the differences in operating conditions and the rapid poisoning of common transition metal catalysts by the nitrogen- and sulfur-containing biogenic impurities present in the broth. Here, we demonstrated the potential of electrochemistry for the hydrogenation of MA, a biologically produced unsaturated C_6 diacid. The MA-containing broth was electrochemically processed under ambient conditions to selectively produce *t*3HDA, a bioadvantaged monomer. Nine parameters critical to the electroorganic synthesis step have been studied, and the corresponding results were integrated in an early stage technoeconomic analysis. The best results were obtained when the fermentation broth was degassed to remove dissolved oxygen and processed in a single-compartment electrochemical reactor using Pb as

a working electrode. A TEA revealed that, under these conditions, *t*3HDA could be produced at approximately \$2.00 kg^{-1}. Using a cheaper feedstock or engineering of the metabolic pathway to achieve higher MA yields and titers from glucose would further decrease the cost of *t*3HDA to just below \$1.00, making biobased *t*3HDA cheaper than petroleum-based adipic acid.

Acknowledgements

Part of this material is based upon work supported in part by National Science Foundation Grants CBET-1512126, EEC-0813570, and EPSC-1101284, and the Plant Sciences Institute at Iowa State University. We would like to thank Dr. Sarah Cady (ISU Chemical Instrumentation Facility) for training and assistance pertaining to the AVIII-600 results included in this publication, Patrick Johnston for assistance pertaining to the ICP-OES results included in this publication, and Xiaotong Chadderdon and David Chadderdon for helpful discussions.

References

1. Choi, S.; Song, C. W.; Shin, J. H.; Lee, S. Y. *Metab. Eng.* **2015,** 28, 223-239.
2. Lane, J. *The DOE's 12 Top Biobased Molecules – What Became of Them?* http://www.biofuelsdigest.com/bdigest/2015/04/30/the-does-12-top-biobased-molecules-what-became-of-them/ (accessed August 6).
3. van Putten, R.-J.; van der Waal, J. C.; de Jong, E.; Rasrendra, C. B.; Heeres, H. J.; de Vries, J. G. *Chem. Rev.* **2013,** 113, 1499-1597.
4. Saha, B.; Abu-Omar, M. M. *Green Chem.* **2014,** 16, 24-38.
5. Gröger, H.; Hummel, W. *Curr. Opin. Chem. Biol.* **2014,** 19, 171-179.
6. Vennestrøm, P. N. R.; Christensen, C. H.; Pedersen, S.; Grunwaldt, J.-D.; Woodley, J. M. *ChemCatChem* **2010,** 2, 249-258.
7. Schwartz, T. J.; O'Neill, B. J.; Shanks, B. H.; Dumesic, J. A. *ACS Catal.* **2014,** 4, 2060-2069.
8. Kroutil, W.; Rueping, M. *ACS Catal.* **2014,** 4, 2086-2087.
9. Shen, Y.; Jarboe, L.; Brown, R.; Wen, Z. *Biotechnol. Adv.* **2015,** 33, 1799-1813.
10. Rover, M. R.; Johnston, P. A.; Jin, T.; Smith, R. G.; Brown, R. C.; Jarboe, L. *ChemSusChem* **2014,** 7, 1662-1668.
11. Lian, J.; McKenna, R.; Rover, M. R.; Nielsen, D. R.; Wen, Z.; Jarboe, L. R. *J. Ind. Microbiol. Biot.* **2016,** 43, 595-604.
12. Cardenas, J.; Da Silva, N. A. *Metab. Eng.* **2014,** 25, 194-203.

13. Xie, D.; Shao, Z.; Achkar, J.; Zha, W.; Frost, J. W.; Zhao, H. *Biotechnol. Bioeng.* **2006,** 93, 727-736.
14. Chia, M.; Schwartz, T. J.; Shanks, B. H.; Dumesic, J. A. *Green Chem.* **2012,** 14, 1850-1853.
15. Schwartz, T. J.; Johnson, R. L.; Cardenas, J.; Okerlund, A.; Da Silva, N. A.; Schmidt-Rohr, K.; Dumesic, J. A. *Angew. Chem. Int. Ed.* **2014,** 53, 12718-12722.
16. Schwartz, T. J.; Shanks, B. H.; Dumesic, J. A. *Curr. Opin. Chem. Biol.* **2016,** 38, 54-62.
17. Suástegui, M.; Matthiesen, J. E.; Carraher, J. M.; Hernandez, N.; Rodriguez Quiroz, N.; Okerlund, A.; Cochran, E. W.; Shao, Z.; Tessonnier, J.-P. *Angew. Chem. Int. Ed.* **2016,** 55, 2368-2373.
18. Matthiesen, J. E.; Carraher, J. M.; Vasiliu, M.; Dixon, D. A.; Tessonnier, J. P. *ACS Sustainable Chem. Eng.* **2016,** 4, 3575-3585.
19. Deinove http://www.deinove.com/en.
20. Myriant http://www.myriant.com/products/product-pipeline.cfm.
21. Bui, V.; Lau, M. K.; Macrae, D. Methods for producing isomers of muconic acid and muconate salts. WO2011085311 A1, July 14, 2011.
22. Johnson, C. W.; Salvachúa, D.; Khanna, P.; Smith, H.; Peterson, D. J.; Beckham, G. T. *Metab. Eng. Commun.* **2016,** 3, 111-119.
23. Xie, N.-Z.; Liang, H.; Huang, R.-B.; Xu, P. *Biotechnol. Adv.* **2014,** 32, 615-622.
24. Olson, D. A.; Sheares, V. V. *Macromolecules* **2006,** 39, 2808-2814.
25. Olson, D. A.; Gratton, S. E. A.; DeSimone, J. M.; Sheares, V. V. *J. Am. Chem. Soc.* **2006,** 128, 13625-13633.
26. Vardon, D. R.; Rorrer, N. A.; Salvachúa, D.; Settle, A. E.; Johnson, C. W.; Menart, M. J.; Cleveland, N. S.; Ciesielski, P. N.; Steirer, K. X.; Dorgan, J. R.; Beckham, G. T. *Green Chem.* **2016,** 18, 3397-3413.
27. Elvidge, J. A.; Linstead, R. P.; Smith, J. F. *J. Chem. Soc.* **1953**, 708-711.
28. Pletcher, D.; Walsh, F. In *Industrial Electrochemistry*, Springer Netherlands: 1993; pp 294-330.
29. Botte, G. G. *Electrochem. Soc. Interface* **2014,** 23, 49-55, 7 pp.
30. Mackenzie, p. W. http://www.pcinylon.com/index.php/markets-covered/adiponitrile.
31. Perlman, N.; Albeck, A. *Synth. Commun.* **2000,** 30, 4443-4449.
32. Bard, A. J.; Faulkner, L. R. *Electrochemical Methods: Fundamentals and Applications*; Masson: 1982.
33. Claypool, J. T.; Raman, D. R. *Bioresource Technol.* **2013,** 150, 486-495.
34. Viswanathan, M. B.; Raman, D. R.; Claypool, J. T.; Squire, M. In *Developing an early-stage cost analysis and lifecycle greenhouse-gas emission estimation tool for Biorenewable Processing – Part I: BioPET to ESTEA*, American Society of Agricultural and Biological Engineers Annual International Meeting, Montreal, Quebec, Montreal, Quebec, 2014.
35. Dysert, L. R. **2003,** 45, 22-30.
36. Mazur, D., ElectroCell North America, Inc.: Personal communication, 2016.
37. iHS *Bio-Based Adipic Acid*; Report 284; 2012.
38. Zhang, Z.; Jackson, J. E.; Miller, D. J. *Bioresource Technol.* **2008,** 99, 5873-5880.
39. Bechthold, I.; Bretz, K.; Kabasci, S.; Kopitzky, R.; Springer, A. *Chem. Eng. Technol.* **2008,** 31, 647-654.
40. Frost, J. W.; Miermont, A.; Schweitzer, D.; Bui, V. Preparation of trans,trans muconic acid and trans,trans muconates. US8426639 B2, June 16, 2010.
41. Schwartz, T.; Brentzel, Z.; Dumesic, J. *Catal. Lett.* **2015,** 145, 15-22.
42. Pourbaix, M. *Atlas of Electrochemical Equilibria in Aqueous Solutions*; Pergamon: 1966.
43. Song, Y.; Gutiérrez, O. Y.; Herranz, J.; Lercher, J. A. *Appl. Catal., B* **2016,** 182, 236-246.
44. In *CRC Handbook of Chemistry and Physics*, 97 ed.; Haynes, W. M., Ed. 2016.
45. Van de Vyver, S.; Roman-Leshkov, Y. *Catal. Sci. Technol.* **2013,** 3, 1465-1479.

46. Organization, B. I. *Advancing the biobased economy: Renewable chemical biorefinery commercialization, progress, and market opportunities, 2016 and beyond*; 2016.
47. LLC, I. S. *Bio-Based Adipic Acid*. http://www.chemengonline.com/bio-based-adipic-acid/?printmode=1#disqus_thread.
48. USDA *Sugarcane of sugar: price per ton, by state*. http://www.ers.usda.gov/datafiles/Sugar_and_Sweeteners_Yearbook_Tables/World_and_US_Sugar_and_Corn_Sweetener_Prices/TABLE13.XLS.
49. Choi, J.-i.; Lee, Y. S. *Bioprocess Eng.* **1997,** 17, 335-342.
50. Kazi, F. K.; Fortman, J. A.; Anex, R. P.; Hsu, D. D.; Aden, A.; Dutta, A.; Kothandaraman, G. *Fuel* **2010,** 89, Supplement 1, S20-S28.
51. Viswanathan, M. B. Technoeconomic analysis of fermentative-catalytic biorefineries: model improvement and rules of thumb. Iowa State University, Ames, Iowa, 2015.
52. Suástegui, M.; Shao, Z. *J. Ind. Microbiol. Biot.* **2016,** 43, 1611-1624.
53. Suástegui, M.; Guo, W.; Feng, X.; Shao, Z. *Biotechnol. Bioeng.* **2016,** 113, 2676-2685.
54. Das, R. K.; Brar, S. K.; Verma, M. In *Platform Chemical Biorefinery*, Elsevier: Amsterdam, 2016; pp 133-157.
55. Humbird, D.; Davis, R.; Tao, C.; Kinchin, C.; Hsu, D.; Aden, A.; Schoen, P.; Lukas, J.; Olthof, B.; Worley, M.; Sexton, D.; Dudgeon, D. *Process design and economics for biochemical conversion of lignocellulosic biomass to ethanol dilute-acid pretreatment and enzymatic hydrolysis of corn stover*; NREL/TP-5100-47764; 2011.
56. Peters, M.; Timmerhaus, K.; West, R. *Plant design and economics for chemical engineers*; McGraw-Hill: New York, 2003.
57. Walas, S. M. *Chemical process equipment selection and design.* ; Butterworth-Heinemann: 1990.
58. Genskow, L. R. *Perry's chemical engineers' handbook. Section 12, Psychrometry, evaporative cooling, and solids drying*; McGraw-Hill: New York, 2008.
59. Towler, G.; Sinnott, R. *Chemical engineering design: principles, practice and economics of plant and process design*; 2nd ed.; Elsevier: 2013.

Supporting Information

Cis-3-hexenedioic acid synthesis

To the solution of cis-3-hexenedialdehyde (1.60 g, 14.3 mmol) in acetone (30 mL) in an ice water bath was added 2.5 mL of 8 M Jones reagent in 25 mL of acetone over a period of 1 h, keeping the bath temperature between 0 °C and 10 °C. After stirring an additional hour, several drops of i-PrOH were added to destroy the excess oxidant. Water was then added and the acetone was then removed via rotary evaporation. The aqueous solution was extracted three times with EtOAc, the organic phase was extracted back with basic water (pH 8 ~ pH 9) and the latter aqueous phase was acidified with concentrated HCl to pH 1. This solution was extracted three times with EtOAc, dried over $MgSO_4$, filtered and evaporated to get the crude diacid. Recrystallization failed to provide pure product. Therefore, charcoal was used to decolorize the crude product and further purification by column chromatography (silica gel, EtOAc) afforded the diacid as a white solid in 58% yield.

Calculations

Conversion, selectivity, and faradaic efficiencies are calculated as follows. I is the current transferred, t is the reaction time, V is the volume of the electrolyte, and F is Faraday's constant. *Cis,trans*-muconic acid (*ct*MA), *trans,trans*-muconic acid (*tt*MA), *trans*-3-hexenedioic acid (*t*3HDA), *cis*-3-hexenedioic acid (*c*3HDA). The initial *tt*MA concentration $[ttMA]_0$ was typically <7 μM.

$$ctMA\ \text{Conversion}\ (\%) = \left(1 - \frac{[ctMA]_t}{[ctMA]_0}\right) * 100 \quad (1)$$

$$t3HDA\ \text{Selectivity}\ (\%) = \frac{[t3HDA]_t}{[ctMA]_0 - [ctMA]_t} * 100 \quad (2)$$

$$c3HDA\ \text{Selectivity}\ (\%) = \frac{[c3HDA]_t}{[ctMA]_0 - [ctMA]_t} * 100 \quad (3)$$

$$\text{AA Selectivity}\ (\%) = \frac{[AA]_t}{[ctMA]_0 - [ctMA]_t} * 100 \quad (4)$$

$$ttMA\ \text{Selectivity}\ (\%) = \frac{[ttMA]_t - [ttMA]_0}{[ctMA]_0 - [ctMA]_t} * 100 \quad (5)$$

$$\text{Faradaic Efficiency}\ (\%) = \frac{([t3HDA]_t * 2 + [c3HDA]_t * 2) * F * V}{I * t} * 100 \quad (6)$$

Technoeconomic analysis with ESTEA

As its name implies, the ESTEA model is a spreadsheet-based static model that provides Class 4 level estimates of cost with Class 5 investments.[35] Costs were calculated as follows:

- Beginning with the overall plant productivity, stage yields are used to determine total feedstock demand, which is then multiplied by feedstock price to obtain total annual feedstock cost.
- Fermentation cost is estimated using overall product flow which is computed by plant size, combined with volumetric productivity. Batch fermentation is assumed, with five 3800 m^3 fermenters supported by 10 seed fermentation vessels.[55] Fermenter cost per unit volume is based on Humbird et al., 2011.[55] We assumed the steam

requirements to be 10% (kg_{steam}/kg_{media}). Nutrients are supplied in the form of corn steep liquor added at a rate of 1% (w/w).

- ESTEA assumes centrifugation immediately after fermentation. Centrifuge sizing is done on an energy per unit volume basis per Peters et al., 2003.[56] For this model, a centrifuge size of 400 kW is estimated, with a based cost of $140k.
- Electrochemical sizing calculations are based upon consultation with an external vendor. We received a quote for a reactor from a vendor, who based the quote on the flow data we provided. This quote was then used for the capital cost. Electrical demand was determined based on the experiments performed in the laboratory. Electrode recovery was set to 99%, though we did not lose much material experimentally. The 1% loss does not impact overall cost as catalyst price is negligible compared to overall costs. Unit throughput and other electrochemical considerations were not considered at this early stage of process development.
- Adsorption is sized using experimentally-determined Freundlich adsorption parameters (coefficient and exponent). The column size is then determined based on the flow, which yields 628 m^3, and an estimated capital cost of $110k.[56] Adsorbent costs are estimated using an activated carbon price of $1.00 kg^{-1} and an adsorbent life of 0.5 year.
- We assume an external forced circulation crystallizer, due to its advantage of continuous operation and high production rate. Sizing and costing is per Walas (1990).[57] A single crystallizer, producing 10,000 kg hr^{-1} of final product was scaled and the chosen equipment was well suited to handle that quantity (max. crystallizer size was – 50,000 kg hr^{-1}) according to Walas, 1990. Dryer requirements to separate and purify the crystallized samples were configured based on Perry's Chemical Engineering Handbook – sections: *Liquid-Solid Systems, Solids Drying and Gas-Solid Systems* (Genskow, 2008). The dryers are scaled to produce 400 kg product/hr at an estimated capital cost of $160k.[58]
- With all the major unit operations sized and costed, we use the Lang factor to compute installed cost. This total installed cost is used as the baseline capital cost for the project, and is subsequently converted into an annual cost via amortization at 10% annual interest rate for 10 years. No taxes, depreciation, or salvage costs are included in this analysis.
- Labor costs are computed for each unit operation, based workers per unit operation per shift.[56, 59] Maintenance and repair are computed as 5% of baseline capital cost, Operating supplies at 3% of baseline capital cost, patents and royalties at 2% of baseline capital cost, general expenses and plant overhead cost are included at 10% of total annual costs.

The corresponding breakdown of the costs is presented in Table S4.

1

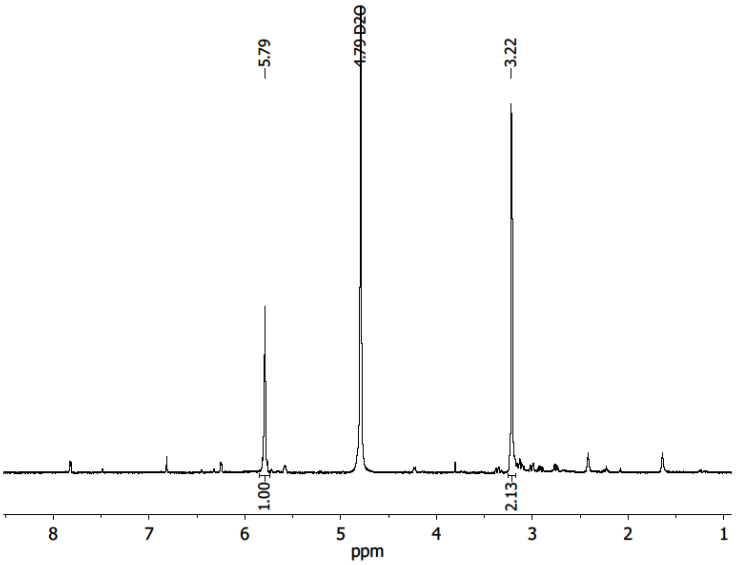

Figure S1. ^{1}H NMR spectra, 600 MHz, D_2O, of *cis*-3-hexenedioic acid (*c*3HDA). Compared to *trans*-3-hexenedioic acid, the signals for *c*3HDA are slightly downfield.

Table S1. Geometric dimensions of the metal electrodes. Rotating disk electrodes (RDE) purchased from pine are 5 mm in diameter.

Metal	Length (mm)	Width (mm)	Thickness (mm)	Area (cm^2)
Pb	22.0	12.7	0.3	5.7
Pb RDE	-	-	-	0.196
Pt RDE	-	-	-	0.196

Table S2. Plasmids used in this work to engineer strain YSG50 for production of MA from glucose through the shikimic acid pathway. See reference [17] for a full description of the plasmid assembly.

Plasmid	Gene cassettes	Description
pRS425- Sc MA	PYKp-*PaAroZ* -ADH2t GPDp-*HQD2*-PYK1t TEF1p-*KpAroY*-HXT7t	Plasmid containing the 3-gene heterologous pathway for MA production from dehydroshikimic acid (DHS).
pRS413 *aro4*$_{K229L}$-*tkl1*	TPI1p-*aro4*$_{K229L}$-TDH1t ADH1p-*TKL1*-ADH1t	Plasmid harboring a tyrosine insensitive *aro4* to avoid feedback inhibition. Also contains the transketolase 1 gene to increase the pool of erythrose-4-phosphate.
pRS426 *aro1*$_{D1409A}$	GPDp-*aro1*$_{D1409A}$-PYK1t	Plasmid harboring the mutant *aro1* gene to halt the conversion of DHS to shikimic acid.

Table S3. Concentrations of trace metal impurities determined by ICP-OES for the recovered *t*3HDA product.

Element	Concentration (ppb)	Concentration in the sample (wt.%)
Calcium (Ca)	130	0.3
Copper (Cu)	below detection limit	-
Iron (Fe)	below detection limit	-
Potassium (K)	10	0.03
Magnesium (Mg)	80	0.2
Sodium (Na)	11	0.03
Lead (Pb)	below detection limit	-
Zinc (Zn)	below detection limit	-
Platinum (Pt)	below detection limit	-

Table S4. Breakdown of costs ($M) among key cost categories, by unit operation. Feedstock dominates the annual costs. Across unit operations, fermentation and purification are similar in magnitude, at approximately 10% each of total cost; in contrast, electrocatalysis is less than 2% of estimated cost.

Unit Operation	**Unit Capital**	**Capital + Lang Fac.**	**Annual Capital**	**Operating (excl. labor)**	**Labor**	**Total Annual**
Feedstock (glucose)	$-	$-	$-	$121.3	$0.9	**$122.2**
Fermentation	$10.0	$50.2	$8.2	$7.5	$2.2	**$17.9**
Separation (centrif.)	$1.3	$6.7	$1.1	$0.5	$0.2	**$1.8**
Catalysis Total	$0.9	$4.7	$0.8	$1.4	$0.5	**$2.6**
Purification I	*$0.1*	*$0.5*	*$0.1*	*$5.5*	*$0.1*	
Purification II	*$2.4*	*$11.9*	*$1.9*	*$9.0*	*$0.1*	
Purification Total	$2.5	$12.4	$2.0	$14.4	$0.2	**$16.7**
Other Expenses					$4.3	**$11.0**
Total	**--**	**--**	**$12.0**	**$145.2**	**$8.2**	**$172.1**